Validation of Simultaneous PET Emission and Transmission Scans

Christopher J. Thompson, Nicole Ranger*, Alan C. Evans, and Albert Gjedde

Positron Imaging Laboratories, McConnell Brain Imaging Centre, Montreal Neurological Institute and Medical Physics Unit, McGill University, Montreal, Canada

A technique for performing simultaneous PET emission and transmission scans is validated in a fluoro-deoxyglucose study. A point source masked into a fan beam of annihilation photons orbits the patient section under study. Coincident events are sorted into two buffers, or rejected, based on the source's position. Both static and dynamic frames of independent and simultaneous studies are compared. The noise effective count rate is reduced to 62% of the value during normal studies. However, the increase in the coefficient of variation in cortical regions is <6%. The RMS difference between profile contours through many brain regions is ~40% higher comparing two simultaneous emission/transmission scans than when the same analysis is performed on independent emission scans. This difference appears to be due to the noise patterns arising from the use of different transmission scans.

J Nucl Med 1991; 32:154–160

Transmission scans are now used routinely with most positron emission tomography (PET) studies to correct for attenuation of the annihilation photons in the patient section being scanned. Improved transmission scan techniques now in use permit these scans to be performed rapidly, with insignificant random (*1*) and scattered (*2*) events to contaminate the attenuation measurement. Orbiting rod sources are now offered on some new PET scanners (*3*). Until recently, the transmission scan had to be performed before injection of long-lived tracers. This required long periods of immobilization or accurate repositioning between transmission and emission scans.

Carson and Daube-Witherspoon (*4,5*) demonstrated a technique in which transmission and emission scans (E/T scans) are performed in rapid sequence. Some activity within the patient slice being scanned is mixed with that from the orbiting rod source. A fraction, about 5% of the events recorded during the emission scan, must be subtracted from the data recorded during the transmission scan. If this is not done, areas of high activity appear less dense. When the attenuation correction is applied, the activity concentration appears lower than it should. To avoid this subtraction, we introduced the masked orbiting transmission source (MOTS). Our source (*6*) is encapsulated between two lead collimators, which shape the coincident photons emanating from it into a thin fan beam in the scanning plane. The lead shields crystals near the source from radiation within the patient section. The residual contamination, 0.5%, of the transmission scan by radiation from the patient slice can be neglected.

This work has since been extended to allow the E/T scans to be acquired simultaneously (*7*). This requires very strict electronic collimation of the source so that only detector pairs that are strictly collinear with the source may accept transmission events. Those that are far from collinear with the source may accept emission events from the patient section. Events recorded by detector pairs nearly collinear with the source are rejected, so that most of the rays are scattered by the lead collimator. We have shown previously that the correct attenuation coefficients for air, water, and bone-equivalent densities are still observed with activity concentrations as high as 80 kBq/cc (over 2 μCi/cc) in a brain-sized phantom. Furthermore, excellent linearity was obtained when the activity concentration measured during simultaneous E/T scans was plotted against that obtained in independent scans, which demonstrated an 80:1 range of activity concentration.

In this paper, we show that this technique can be used for attenuation correction during static fluorodeoxyglucose (FDG) studies and at least during the latter frames of dynamic studies. This would be especially advantageous in a busy PET center where patient throughput could be improved and all possibility of registration errors eliminated. Carson (*5*) reported a series of six FDG studies where both preinjection and emission-corrected transmission scans were performed. By subtracting transmission scans performed 40 min apart, significant patient movement was demonstrated in three subjects. Since these subjects were restrained in

Received Mar. 20, 1990; revision accepted Jul. 16, 1990.

For reprints contact: C.J. Thompson, DSc, Montreal Neurological Institute, Research Computing Laboratory, 3801 University St., Montréal Quebec, Canada H3A 2B4.

*Current address: Hospital of the University of Pennsylvania, Philadelphia, Pennsylvania.

a thermo-plastic face mask (True-Scan Imaging, Annapolis, MD), one can assume that registration errors are quite common.

To validate this technique, we compared the glucose utilization rate observed during independent and simultaneous E/T scans. Previous work has shown that the operational equation for glucose utilization gives results that are almost independent of time, after the initial uptake of the tracer (*8,9*). We chose to do one extended study in a control subject who was prepared to lie "perfectly still" for 4 hr. During the study, we alternated between independent and simultaneous E/T scans. In this way, the same injection of tracer could be used, eliminating intersubject variability and environmental influences on the metabolic rate.

MATERIALS AND METHODS

The studies were performed on the Positome IIIp (*10,11*) three-slice PET scanner at the Montreal Neurological Institute. The scanner has two rings of 64 BGO crystals and an efficiency of 70K cps (μCi/cc) for each slice. The technique for acquiring simultaneous E/T scans has been described in detail (*7*) and has since been extended to allow multiple frames of emission data to be acquired during a single transmission scan. At the time this study was performed, the activity in each transmission source was ~7 MBq (190 μCi). The same transmission sources were used in all studies.

Summary of Simultaneous E/T Technique

During the scan, the collimated point MOTS sources orbit the patient aperture, stopping in front of each of the 64 crystals. After one 2-sec wobble cycle, the source moves to the next crystal. After one orbit, the detector array is rotated (to and fro) over half the inter-crystal angle. The stepwise movement, and necessity for complete wobble cycles before the source moves, impose a minimum frame time of 256 sec. No data are lost during source movement. This currently prevents E/T scans from being performed during the early, short frames of a dynamic study.

The data acquisition hardware sorts events into uniformly spaced parallel projections (*12*). The source angle is subtracted from the projection angle for each event. A look-up table is then used to steer the events into the emission or transmission histogram or reject them entirely.

The average efficiency of each slice during simultaneous E/T scans is 70% of emission-only scans. The data acquisition program compensates the emission data for this and a slight nonuniformity across the field of view. It multiplies data in each column of the sinogram by a relative efficiency factor before storing it on disk. These factors, which were calculated during the programming of the look-up table (*7*), compensate for higher scattering from the lead surrounding the source near the edge of the field of view. The emission sinograms can, thus, be reconstructed without further special treatment.

Separate files are created for both emission and transmission events. If there is no couch movement between emission frames, acquisition of transmission data is continued in the same frame. When the couch moves for fuller brain coverage, separate transmission data frames are collected.

The transmission sinograms are divided into data acquired during a blank field scan. The blank scan is performed once a week for 4096 sec to reduce the noise associated with the blank scan. The resulting data are used for attenuation correction and can be reconstructed into an atenuation scan. The program, which formats the attenuation scan data, can subtract any fraction of the simultaneous emission scan.

Control Subject Selection, Preparation, and Scanning Sequence

The study was performed on a 23-yr-old male student who gave consent knowing that he would have to lie perfectly still for up to 4 hr. After inserting a catheter in his left radial artery, his head was immobilized in a tight-fitting foam mold.

The scanning protocol, shown in Table 1, started with full brain coverage with a preinjection transmission scan. A slow injection of 185 MBq (5 mCi) of FDG was made into the radial vein. The initial sequence of our standard FDG dynamic sequence was followed until the frame time was of sufficient length to allow simultaneous E/T scans to start. Alternate emission-only and E/T scans were performed over a period of 2.5 hr. It took ~1 min during each change from emission-only to E/T scanning. We had to remove or insert the source, reposition the bed, and change acquisition programs. Otherwise the scanning was continuous.

Dynamic Study Data Analysis

All emission-only studies were reconstructed with the preinjection attenuation correction. E/T emission scans were reconstructed with their companion attenuation scan. The first 25 min of the dynamic study, with slices at 0, 18, 36 mm above the orbital-meatal (OM) line, was combined with the data from all other studies in those planes into one file covering 2 hr after injection. Since this sequence includes three periods during which we scanned higher slices, the full dynamic scan sequence has two gaps of 25 min.

For the last nine frames in this study, we tabulated the total true counts per slice and the random count fraction, which are the bases for assessment of relative image noise. The slice efficiency, live time, and random fraction depend on the type of scan and the time after injection. To account for this, we also calculated the noise-effective counts (NEC) according to the formula:

$$NEC = \frac{T}{(1 + R/T + S/T)},$$

where T is the true counts (before live time correction), R/T is the random count fraction, and S/T is the scattered count fraction. These quantities are all calculated during the reconstruction of each slice.

We examined time-activity curves (TACs) for 12 cm^2 regions of interest (ROIs) in both inferior temporal lobes. These regions were chosen for their homogeneity as determined by their low coefficient of variation (COV) in the longest frames. A central region with a very high COV, representing the "worst case," was also examined. The display program calculates the COV within each ROI to allow fitting programs to weight each time point according to the relative noise. Each region's COV was plotted against time to examine how the simultaneous transmission scan increases the noise in a ROI. Since the efficiency is reduced to 70%, and the random counts increase during transmission scans, the COV must increase.

Static Study Data Analysis

We reconstructed each set of static frames, the early E/T, emission-only, and late E/T, using the three transmission scans acquired during the preinjection and those during the early and late E/T scans. These images were scaled to regional glucose utilization rate, using the plasma TAC and standard rate constants. In the nine image sets, we selected slice 8, 61 mm above the OM line, for contour profile analysis.

Using our ROI program (*13*), a line was drawn, starting on the medial aspect of the frontal cortex, forward to the frontal pole, then posterior following the cortical rim. It continued through the temporal, parietal, and occipital cortex, into the medial occipital cortex, across the lateral ventricle, and through the thalamus and striatum. Figure 1 shows the profile drawn on the early E/T slice.

We chose the emission-only study reconstructed with the preinjection attenuation scan as the reference contour. To assess the difference between these contour profiles, we measured the difference in the arithmetic mean of the glucose utilization rate. We then calculated the RMS difference between points on each contour and the reference contour. For comparison, we performed a similar analysis on a slice 36 mm above the OM line in which three emission-only scans were performed. These scans were reconstructed by summing two frames of the dynamic study starting at 20 and 40 min. Scans at 20 and 89 min were compared with a reference at 40 min.

TABLE 1
Protocol for Validation of Simultaneous E/T Scans

−60	min: Subject positioned on Positome couch and head mold made to allow scanning at the OM line; arterial line installed.
−40	min: Four frames of preinjection transmission scans for 512 sec, moving couch between scans for full brain coverage. Total time 34 min.
−5	min: Venous catheter installed for injection of FDG.
0	min: Injection of FDG. Independent emission acquisition of 25-min dyanmic study. Lower slice at OM line. Frames times: 10 of 30 sec, 10 of 60 sec, 2 of 256 sec.
26	min: Two emission frames of 256 sec, during one transmission scan of 512 sec.
40	min: Two independent emission frames of 256 sec.
60	min: Four frames of simultaneous E/T scans for 512 sec, moving couch between for full brain coverage. Total time 34 min.
95	min: Four frames of independent emission scans for 512 sec, moving couch between scans for full brain coverage. Total time 34 min.
120	min: Four frames of simultaneous E/T scan for 512 sec, moving couch between for full brain coverage. Total time 34 min.
155	min: End of study. Total time for subject is 3.5 hr.

Assessment of Effect of Emission Scan Subtraction

We have previously shown (*7*) that there is about 0.5% contamination of the transmission scan by activity in the section being examined. We assessed the magnitude of this contamination in a typical imaging situation where E/T scans would be most useful. The program, which formats the transmission scan into an attenuation file, allows the user to specify the fraction of the simultaneous emission scan to be subtracted. This is done before dividing the transmission data into the blank field data. In all other studies reported here, we subtracted 0.5% of the emission scan. Here, we also used an attenuation file without emission scan subtraction. Both attenuation files were used during the reconstruction of the early E/T scan. Slice 8 was then subject to the same profile analysis described previously.

RESULTS

Dynamic Study

The imaging parameters that allow an estimate of the relative image noise for six frames of the dynamic study are given in Table 2. In order to represent the same imaging time in each period, the first three periods represent the sum of two 256-sec dynamic frames. The first three periods were separated by 10 min during which time the uptake was almost balanced by the isotope decay. During the E/T scan, the random counts increased from 5% to 20%, and the live time dropped from 95% to 88%. These factors, plus the reduced efficiency, combine to yield an effective count rate during the E/T scan of 62% of the average emission-only scan. The last three scans were 30 min apart. In the last E/T frame, the random fraction rose to 36% as the fluorine-18 had decayed significantly by this time.

The 30 frames of the dynamic sequence for a slice 18 mm above the OM line are shown in Figure 2. Three regions were identified and TACs for these regions superimposed on the images. The E/T frames were marked with the letter T. The effect of the noise is easily seen in Figure 3, which shows the COV plotted for the regions in Figure 2. The hatched background in three regions shows where transmission scans were recorded. The mid-line region showed a sharp increase in noise during these periods. There was only a minimal effect in the cortical regions.

Static Studies

Figure 4 shows three slices comparing independent and simultaneous scans. These images were reconstructed with a filter matched to the detector's spatial frequency response, producing an image resolution of 12 mm full width at half maximum. The images are sections 0, 25, and 61 mm above the OM line. While every effort was made to reduce subject movement, many of the slight differences in these scans are clearly due to misregistration. This is most noticeable in the middle slice of the transmission scans. The areas of different density in the anterior regions are the superior

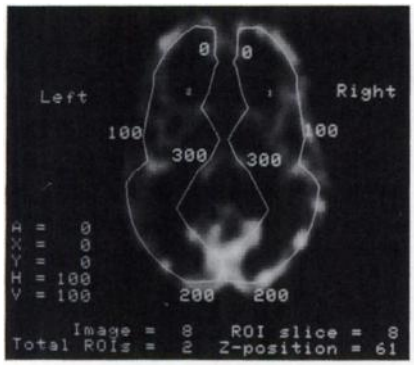

FIGURE 1
Profiles on the left and right hemispheres of a slice 61 mm above the OM line. The numbers are distances in mm along the profile to locate structures in Figure 5.

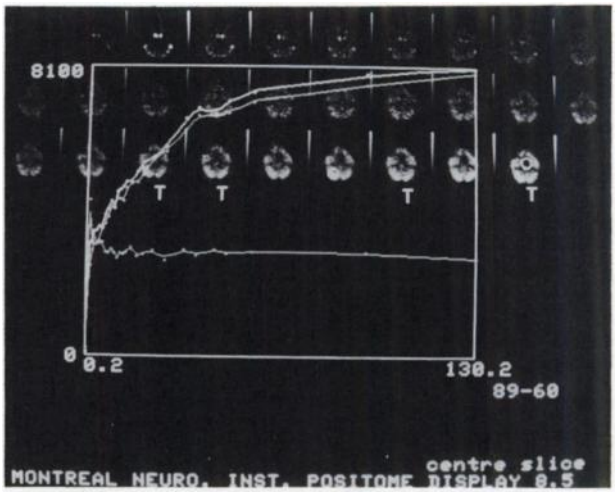

FIGURE 2
Series of frames from a slice at the OM line showing the time sequence of FDG uptake over a period of over two hours. The images marked "T" were acquired during a transmission scan. The overlays represent TACs from two cortical and one mid-line ROI.

regions of the sinus and bony ridge behind the eyes, suggesting that the subject may have tilted his head back between these studies.

Figure 5 shows the contour profiles along the line drawn in Figure 1 in the right hemisphere. It shows the early simultaneous, the independent, and late simultaneous contour profiles. The numbers next to the line-style keys shows the mean glucose utilization for the profile and the RMS difference from the independent scan. The values for the same contour are given for all reconstructions of these studies in Table 3. Each profile is compared to the independent emission scan reconstructed with the preinjection transmission scan.

Figure 6 shows a similar profile analysis performed on three emission-only slices. A slice 36 mm above the OM line was chosen as the higher slice had only one emission-only study. The calculated glucose utilization was much lower in the scan performed at 20 min after injection. (This was considered to be too early in the study for the FDG model to be independent of the rate constants (*8*) and was not used for comparison with the E/T scans.) The other two contours are quite consistent. The means and difference for this and a region on the right side are given in Table 4. The mean difference was 1 μmole/100 g/min in observed glucose utilization rate between the two latter studies, which is the same as that seen in the E/T studies. The RMS differences for the emission-only studies are 60% of the values in Table 3, suggesting that they are more consistent. This is not an unexpected finding since they were reconstructed with the same transmission scan.

Figure 7 shows profiles for the right hemisphere in the same slice analyzed in Figure 5. Here the slice is reconstructed with and without subtraction of the 0.5%

TABLE 2
Imaging Parameters Observed During Emission-Only and E/T Scans

Start time (min)	Scan true type counts (*1000)	Random counts (%)	Live time (%)	Noise-Eff counts (*1000)
20	E 1633	5	95	1269
30	E/T 1026	21	88	722
40	E 1416	5	95	1081
51	E/T 931	21	89	655
89	E 981	4	96	755
97	E/T 475	36	90	334

The first three lines are the sums of two 256-sec emission frames. The others are 512-sec frames. The true counts column includes the effect of live time and reduced efficiency during the E/T scans. It does not include scattered counts or randoms from the random count column. The noise-effective counts column represents the effective counts after compensating for scatter and randoms.

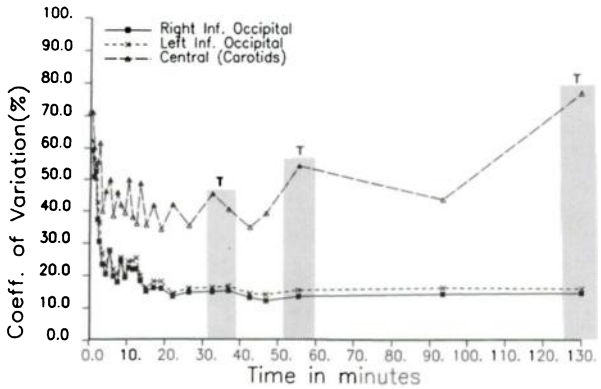

FIGURE 3
The coefficients of variation of each point in the TACs in Figure 2 are plotted against time. The regions in the hatched background were recorded during a transmission scan.

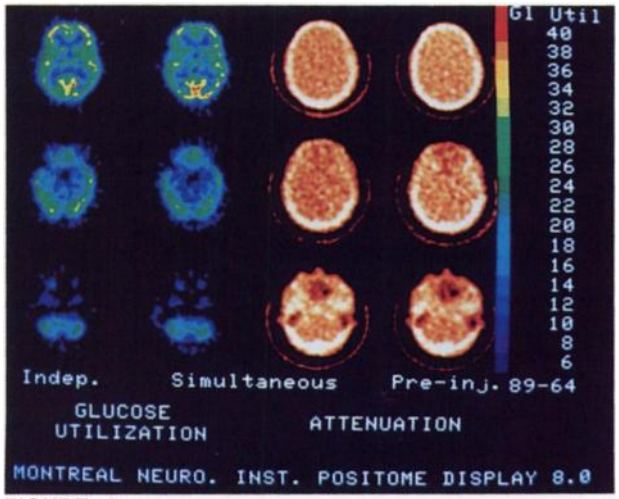

FIGURE 4
Typical images of independent emission, simultaneous emission and transmission, and preinjection transmission scans at 0, 25, and 61 mm above the OM line.

contamination of the transmission scan by the emission data. The mean glucose utilizations of these contours are 26.34 and 26.25 μmole/100 g/min. These contours are very close to each other, showing that this contamination is probably negligible. When extra events are recorded during the transmission scan, the observed attenuation correction will be smaller. When this correction is applied during the reconstruction of the emission scan, the activity concentration appears less than it should.

DISCUSSION

The work reported here represents the situation in which E/T studies would be most beneficial in reducing the time a patient must spend in the scanner during a PET study. To study the potential errors introduced by this new scanning mode, it was necessary to subject a volunteer to a study much longer than normal.

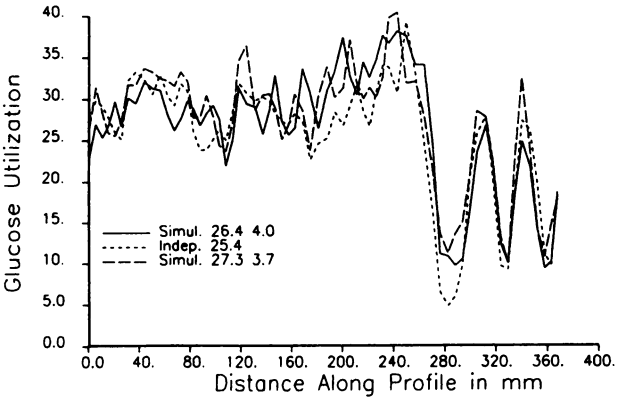

FIGURE 5
Contour profiles through the right hemisphere in a slice 61 mm above the OM line. The three contours are for the early E/T, the emission-only, and late E/T study.

Our analysis of the noise effective counts in different frames shows that the effective efficiency of the scanner is reduced to 62% during E/T scans. This includes the effects of randoms and reduced live time as well as the data segmentation into emission and transmission files. The increase in noise can be weighed against the systematic errors caused by misregistration (*14*) of the E/T scans which can occur during normal scanning.

The regional analysis of the dynamic data represents a typical starting point for the estimation of rate constants, etc. from TACs. The two cortical regions represent areas of relatively high activity concentration. These were affected comparatively less by any noise or bias introduced by the simultaneous transmission scans. The mid-line region, the lower curve in Figure 2, represented the "worst-case" situation for image noise. There was only a significant activity concentration in the early frames from the high concentration in the carotid arteries. Since random counts are uniformly spread over the field of view and there are more randoms during a transmission scan, the noise was greater there.

From the theory of noise propagation in reconstructed images (*15*), one would expect a proportionately higher signal-to-noise ratio in regions of high activity than if these were planar images from a gamma camera. This is well demonstrated in the analysis of dynamic data. In spite of a lower effective count-rate during the E/T scans, the COV increased only 6% in the cortical regions. In a region where there was negligible activity, the COV increased by up 12% in early frames and 50% in later frames.

In the contour analysis of the static studies, we see a greater difference between the E/T and independent scans than that observed when comparing two emission-only studies. Part of the difference is due to the noise added during any transmission scan. In homogenous regions, transmission scans show a mottled pattern which will be different for each independent scan. An artificially radiolucent region in one transmission scan could have normal density in the next study. This density change is reflected into the emission scan as increased noise.

Other contributions include the use of extended times after the injection of FDG and the fact that our profiles enter a heterogeneous tissue mix. We have used the standard gray matter rate constants in our analysis. The scanner's couch repositioning accuracy is ±2 mm. The emission-only study analyzed here is actually 3 mm below the E/T studies.

The difference in contours, with and without correction for crosstalk from the emission scans, is very small due to the lead mask surrounding the source. In the technique of Carson et al. (*4,5*), where no lead sur-

TABLE 3
Summary of Results of Profile Contour Analysis in a Slice 61 mm Above OM Line

	Glucose Metabolic Rate					
	Emission Scan Type and Time					
	Left			Right		
	Simultaneous early	Independent	Simultaneous late	Simultaneous early	Independent	Simultaneous late
Time after injection	79 min	115 min	153 min	79 min	115 min	153 min
Attenuation correction						
Early simultaneous	23.9	26.2	25.6	26.3	27.6	27.9 Ave.
	−1.0	+1.3	+0.7	+0.9	+2.2	+2.5 Diff.
	3.4	2.6	2.9	4.0	3.3	4.2 RMS
Preinjection independent	22.5	24.9	24.5	24.3	25.4	26.1 Ave
	−2.4	—	−0.4	−1.1	—	+0.7 Diff.
	3.1	—	2.4	2.6	—	2.6 RMS
Late simultaneous	23.1	25.6	25.2	25.3	26.6	26.1 Ave.
	−2.5	+0.7	+0.3	−0.3	+1.2	+0.7 Diff.
	3.6	2.4	3.2	3.5	2.7	2.5 RMS

The three emission scans of this slice were reconstructed with three different attenuation scans. The values in the table show the mean glucose utilization in the profile, the arithmetic difference from the reference scan (independent emission and preinjection transmission), and the RMS difference from the reference scan.

rounds the source, the crosstalk is 10 times higher than that measured previously (*7*). In the Carson technique, subtraction of the appropriate fraction of the emission scan is essential.

Our MOTS technique would be improved upon in a scanner with higher intrinsic resolution and lower sensitivity to random counts. The Positome has an intrinsic resolution of 11 mm. On a high resolution scanner, the source tracking could be improved, reducing the extent of the rejection band, and improving the emission efficiency during E/T scans.

The lower limit of the emission frame time is caused by our implementation of the technique and is not intrinsic. The only absolute requirement is that the transmission source must make an integral number of full orbits during each frame of the emission scan. We force the source to stop in front of each detector to maximize the resolution of the transmission scans. It also reduces crosstalk by improved source tracking. On a newer scanner, especially one without detector wobble, the source could orbit once per second, allowing dynamic frames that were any multiple of one second. If the detectors wobble, the source movement would have to be locked to the wobble period to obtain consistent data in each bin of the sinogram.

In most PET scanners, the strongest practical source is normally used for transmission scans to save time

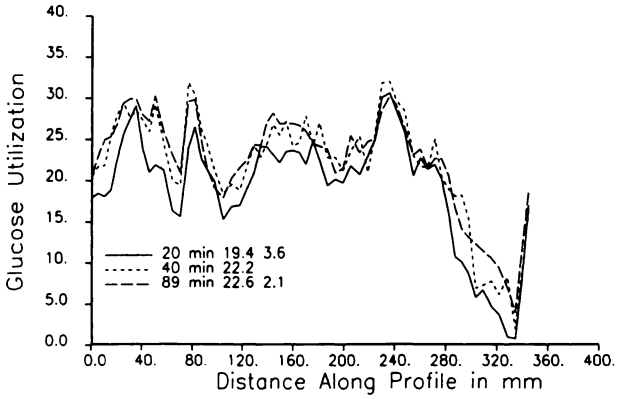

FIGURE 6
Contour profiles through cortex of right hemisphere in three emission-only studies recorded at 20, 40, and 89 min after injection. The slice is 36 mm above the OM line.

TABLE 4
Summary of Results of Profile Contour Analysis for Three Independent Emission Scans of 8.5 Min Duration and Different Starting Times

	Glucose metabolic rate		
	Emission scan start time		
Side	20 min	40 min	89 min
Left profile	18.7	21.9	22.9 Ave.
	−3.2	—	+1.0 Diff.
	3.9	—	2.3 RMS
Right profile	19.4	22.2	22.6 Ave.
	−1.8	—	+0.4 Diff.
	3.6	—	2.1 RMS

The values in the table show the mean glucose utilization in the profile, the arithmetic difference from the reference scan, and the RMS difference from the reference scan.

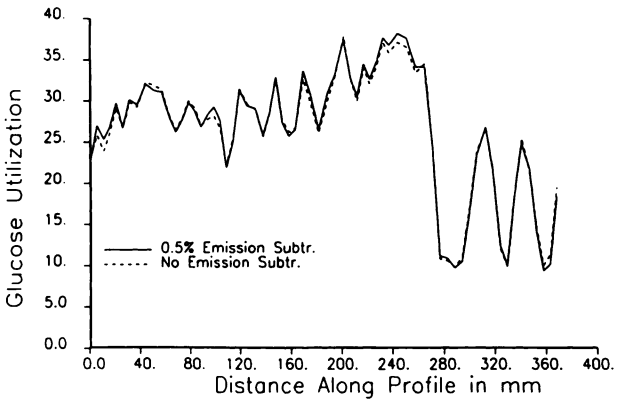

FIGURE 7
Contour profiles for the right hemisphere in a slice 61 mm above the OM line showing the effect of correction of the transmission scan for activity within the subjects's brain.

and reduce transmission scan noise. However, the source strength requirements for E/T scans are quite different from conventional transmission scans. The lower the transmission source strength, the lower the random counts and dead time in the emission scan. If the transmission scan was performed throughout a dynamic uptake study, a weak source could give excellent transmission scans without adding much noise to the emission study.

The activity concentration in the final frames is half that in the first E/T scans. Our earlier phantom studies showed (7) that much wider range of activity concentrations could be used with this technique. We have also performed fluorine Fluro-DOPA E/T studies successfully. Since there is not the same trapping of metabolites of this compound equivalent in the FDG model, DOPA studies would not be useful to validate the technique. No carbon-11 compounds have been used in E/T scans so far. The technique is probably not appropriate for oxygen-15-labeled compounds since the scan times with these compounds are usually much shorter than those normally used for transmission scans.

CONCLUSION

We have demonstrated that simultaneous E/T scans can be used for determining patient slice attenuation and tracer uptake during the same PET scan. These studies have been shown to be practical for a long-lived tracer like FDG because of the advantages of reducing scanning time and improving patient comfort and throughput.

ACKNOWLEDGMENTS

The authors thank the MNI Positron Imaging Laboratory's technical staff, especially Mr. M. Mazza for modifications to the Positome data acquisition electronics. The encouragement of Dr. A. Hakim was very much appreciated.

This work was supported by Program Grant PG41 from the Medical Research Council of Canada, and was presented in part at the SNM Annual Meeting, June 1989, St. Louis, MO.

REFERENCES

1. Carroll LR, Kertz P, Orcut G, The orbiting rod source: improving performance in PET transmission correction scans. In: Esser PD, ed. *Emission computed tomography: current trends.* New York: Society of Nuclear Medicine; 1983.
2. Thompson CJ, Dagher A, et al. A technique to reject scattered radiation in PET transmission scans. In: Nalcioglu O, Cho ZH, Budinger TF, eds. *International workshop on physics and engineering of computerized multidimensional imaging and processing*, Proc SPIE-671;1986:244–253.
3. Kubler WK, Ostertag H, Hoverath H, et al. Scatter suppression by using a rotating pin source in PET transmission measurements. *IEEE Trans Nucl Sci* 1988;NS-35:749–752.
4. Daube-Witherspoon M, Carson RE, Green MV. Postinjection transmission attenuation measurements for PET. *IEEE Trans Nucl Sci* 1988;NS-35:757–761.
5. Carson RE, Daube-Witherspoon M, Green MV. A method for postinjection PET transmission measurements with a rotating source. *J Nucl Med* 1988;29:1558–1567.
6. Ranger NT, Thompson CJ, Evans AC. The application of a masked orbiting transmission source for attenuation correction in PET. *J Nucl Med* 1989;30:1056–1068.
7. Thompson CJ, Ranger NT, Evans AC. Simultaneous transmission and emission scans in positron emission tomography. *IEEE Trans Nucl Sci* 1989;NS-37:1011–1016.
8. Phelps ME, Huang SC, Hoffman EJ, Selin C, Sokoloff L, Kuhl DE. Tomographic measurement of local cerebral glucose rate in humans with (F-18)-2-fluoro-2-deoxyglucose: validation of the method. *Ann Neurol* 1979;6:371–388.
9. Jovkar S, Evans AC, Diksic, Nakai H, Yamamoto YL. Minimization of parameter estimation errors in dynamic PET: choice of scanning schedules. *Phys Med Biol* 1989;34:895–908.
10. Thompson CJ, Yamamoto YL, Meyer E. Positome II: a high efficiency positron imaging device for dynamic brain studies. *IEEE Trans Nucl Sci* 1979;NS-26:583–589.
11. Thompson CJ, Dagher A, Meyer E, Evans AC. Imaging performance of a dynamic positron emission tomograph: Positome IIIp. *IEEE Trans Med Imag* 1986;MI-5:184–198.
12. Dagher A, Thompson CJ. Real-time data rebinning in PET to obtain uniformly sampled projections. *IEEE Trans Nucl Sci* 1985;NS-32:811–817.
13. Evans AC, Beil C, Marrett, et al. Anatomical-functional correlation using an adjustable MRI-based region-of-interest atlas with positron emission tomography. *J Cereb Blood Flow Metab* 1988;8:513–530.
14. Huang S-C, Hoffman EJ, Phelps ME, Kuhl DE. Quantitation in positron emission tomography. 2. Effects of inaccurate attenuation correction. *J Comput Assist Tomogr* 1979;3:804–814.
15. Budinger TF, Derenzo SE, Greenberg WL, Gulbert GT, Huesman RH. Quantitative potentials of dynamic emission computed tomography. *J Nucl Med* 1978;19:309–315.